



Elevated temperature tensile properties and thermal expansion of CNT/2009Al composites

Z.Y. Liu, B.L. Xiao, W.G. Wang, Z.Y. Ma*

Shenyang National Laboratory for Materials Science, Institute of Metal Research, Chinese Academy of Sciences, 72 Wenhua Road, Shenyang 110016, China

ARTICLE INFO

Article history:

Received 4 March 2012

Received in revised form 20 June 2012

Accepted 31 July 2012

Available online 9 August 2012

Keywords:

A. Carbon nanotubes

A. Metal–matrix composite

B. Thermal properties

E. Powder processing

Friction stir processing

ABSTRACT

1.5 vol.% and 4.5 vol.% carbon nanotubes reinforced 2009Al (CNT/2009Al) composites with homogeneously dispersed CNTs and refined matrix grains, were fabricated using powder metallurgy (PM) followed by 4-pass friction stir processing (FSP). Tensile properties of the composites between 293 and 573 K and the coefficient of thermal expansion (CTE) from 293 to 473 K were tested. It was indicated that load transfer mechanism still takes effect at temperatures elevated up to 573 K, thus the yield strength of the 1.5 vol.% CNT/2009Al composite at 423–573 K, was enhanced compared with the 2009Al matrix. However, for the 4.5 vol.% CNT/2009Al composite, the yield strength at 573 K was even lower than that for the matrix, due to the quicker softening of ultrafine-grained matrix. Compared with the 2009Al matrix, the CTEs of the composites were greatly reduced for the zero thermal expansion and high modulus of the CNTs and could be well predicted by the Schapery's model.

© 2012 Elsevier Ltd. All rights reserved.

1. Introduction

The rapid development of the aerospace industry demands that the materials used in instrumental structures be lightweight, high stiffness, and highly thermostable. Aluminium matrix composites with a high elastic modulus, low coefficient of thermal expansion (CTE), and good elevated-temperature mechanical properties, are preferred in those structures which undergo environmental temperature variations between -123 and 473 K in space.

With extremely high elastic modulus (>1 TPa) and high strength (30–100 GPa) [1–5], as well as low CTE (≈ 0) [6], carbon nanotube (CNT) is the most attractive reinforcement for lowering the CTE of the aluminium alloys, as well as for enhancing their elevated-temperature tensile strength. Most previous research efforts have focused on the room tensile properties of the CNT reinforced aluminium matrix composites [7–9], whereas their thermal expansion and elevated temperature tensile properties have been rarely investigated. A fundamental reason for this is the difficulty in incorporating a higher content of CNTs into the aluminium matrix in order to fabricate the composites with sound mechanical properties. Deng et al. [10] reported a 12% reduction in the CTE for a 1.28 vol.% CNT/2024Al composite compared with the Al matrix, but no CTE investigation was conducted on a composite with higher CNT concentrations.

To disperse the CNTs into the metal matrix is a challenge, as the CNT is prone to aggregating as a result of the extremely strong van

der Waals force and its large aspect ratio [11]. Many methods have been developed to incorporate the CNTs into the metal matrix, among these, the two most important methods are ball milling [9,12] and CNT pre-treatment [8,13,14]. However, the CNTs would be severely damaged during milling [15], and with CNT pre-treatment, the CNT concentration is hardly increased, commonly remaining less than 1 vol.% [8,13,14].

Friction stir processing (FSP) is a relatively new metal-working technique (Fig. 1). A non-consumable rotating tool with a specially designed pin and shoulder is inserted into a work-piece and moved along the desired path to cover the region of interest. The combination of tool rotation and translation results in severe deformation and thorough mixing of the material in the processed zone, achieving localised microstructural modification for specific property enhancement.

FSP has been demonstrated to be an effective method of incorporating the reinforcing particles, e.g., nano-sized particles, into the metal matrix and homogenising the microstructure of heterogeneous materials, such as cast alloys and composites [16–18]. Johannes et al. [19] and Morisada et al. [20] fabricated CNT/aluminium alloy composites using FSP. They inserted the CNTs into the holes or grooves which were pre-machined on the aluminium plates and then subjected the plates to FSP. Their results indicated that the HV hardness of the aluminium alloys was increased after incorporating the CNTs by FSP. However, the CNT concentration could not be accurately controlled by pre-setting the CNTs into the holes or grooves. Furthermore, no reports of the tensile properties of the composites were included in their studies.

* Corresponding author. Tel./fax: +86 24 83978908.

E-mail address: zyyma@imr.ac.cn (Z.Y. Ma).

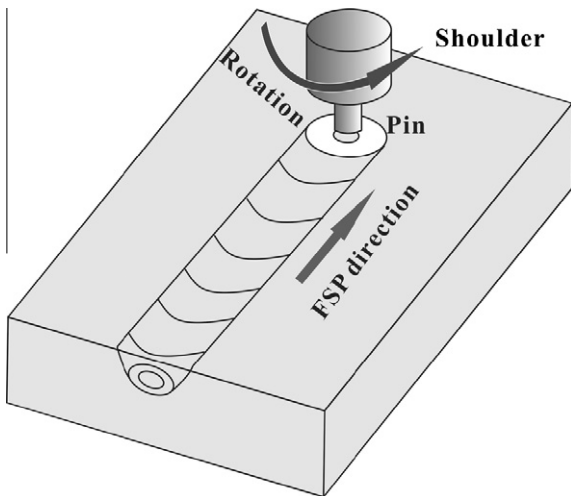


Fig. 1. The schematic of friction stir processing.

In our previous study [21], the CNT/2009Al composites reinforced with CNTs to 4.5 vol.% were successfully fabricated by a combination of powder metallurgy (PM) and FSP. The CNT/2009Al composites exhibited a uniform dispersion of the CNTs and a considerably improved room-temperature tensile strength. This makes it possible to evaluate the CTE and elevated-temperature mechanical properties of the CNT/Al composites. In this work, 1.5 vol.% and 4.5 vol.% CNT/2009Al composites, fabricated using the PM technique and subsequent FSP, were subjected to elevated temperature tension and CTE measurements to understand the elevated-temperature strengthening mechanism of the CNT/Al composites.

2. Experimental procedures

2.1. Raw materials and composite fabrication

The as-received CNTs (95–98% purity) provided by Tsinghua University had an entangled morphology with an outer diameter of 10–30 nm and a length of several microns (Fig. 2a). No extra pre-treatment was conducted on the CNTs. 1.5 vol.% and 4.5 vol.% CNTs were mixed, with 2009Al powders (shown in Fig. 2b, average diameter of 10 μm , nominal composition of Al–4.5 wt.% Cu–1.2 wt.% Mg) in a bi-axis rotary mixer at 50 rpm for 8 h, with a 1:1 ball to powder ratio.

The as-mixed powders were cold-compacted in a cylinder die, degassed and hot-pressed into cylindrical billets with a diameter

of 55 mm and a length of 50 mm. The billets were then hot forged in a steel can at 723 K into disc plates with a thickness of about 10 mm. The plates were subjected to 4-pass FSP at a tool rotation rate of 1200 rpm and a traverse speed of 100 mm/min. A tool with a concave shoulder 20 mm in diameter and a threaded cylindrical pin 6 mm in diameter and 4.2 mm in length was used. For comparison, unreinforced 2009Al was also fabricated using the same method.

2.2. Characterisation of the composites

The as-FSP composites and 2009Al were subjected to a T4-treatment (solutionised at 768 K for 2 h, water quenched and then naturally aged for 4 days). The macroscopic CNT distribution in the matrix, under various fabrication conditions were examined using scanning electron microscopy (SEM, Quanta 600). The microscopic CNT distributions and grain sizes of the composites were observed using transmission electron microscopy (TEM, Tecnai G2 20). The CNTs were extracted from 4.5 vol.% CNT/2009Al composite by using hydrochloric acid, then were examined under TEM.

Tensile specimens with a gauge length of 2.5 mm, a width of 1.5 mm and a thickness of 0.8 mm were machined from the FSP samples perpendicular to the FSP direction. The tensile specimens were held at each test temperature for 20 min and then tested at temperatures of 293–573 K at a strain rate of $1 \times 10^{-3} \text{ s}^{-1}$ on an Instron 5848 tester. The fracture surfaces of the composites were observed on a field emission SEM (Leo Supra).

Thermal expansion specimens with a diameter of 5 mm and a length of 20 mm were machined from the FSP composites along the FSP direction. Linear CTE was measured using a thermal expansion instrument DIL 402 PC at a heating rate of 5 K/min. All the CTE specimens were tested from 293 to 473 K.

3. Results and discussion

3.1. Microstructure of the composites

Fig. 3 shows the SEM images of CNT distributions in 4.5 vol.% CNT/2009Al composites. For the forged CNT/2009Al composite, obvious CNT clusters with a size of about 5 μm were observed and almost no aluminium could be found inside the clusters. This is mainly attributed to the large aspect ratio of the CNTs and the large van der Waals force among the CNTs. This indicates that a common PM process is not effective in dispersing the CNTs into the aluminium matrix, even after forging. After 4-pass FSP, almost no CNT clustering, nor micro-pores could be found in the composites, at least under SEM, which implies that the CNTs were dispersed into the aluminium matrix.

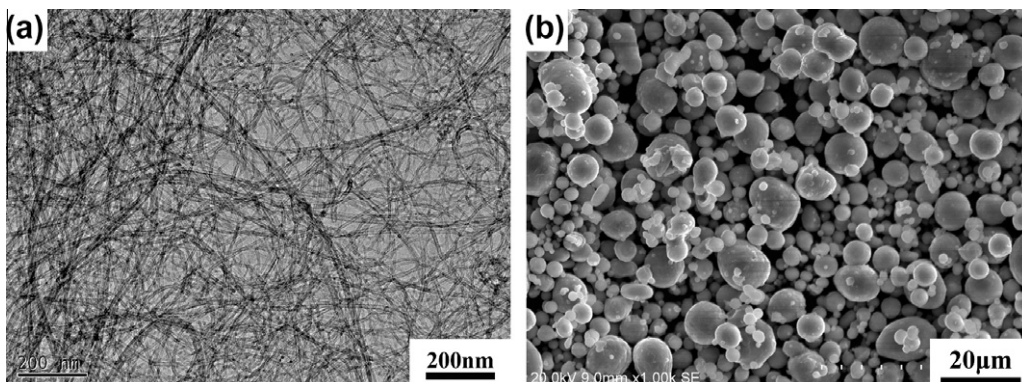


Fig. 2. Morphologies of as-received (a) CNTs and (b) 2009Al powders.

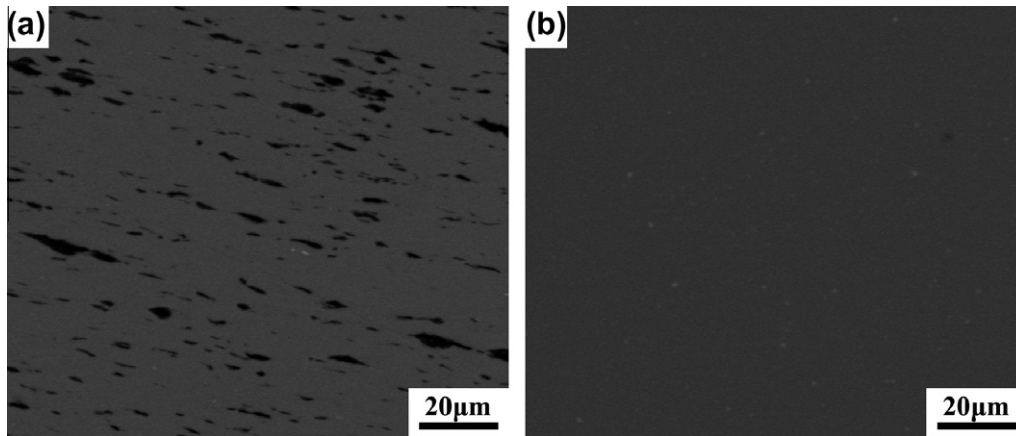


Fig. 3. CNT distribution in (a) forged and (b) FSP 4.5 vol.% CNT/2009Al composites.

Fig. 4 shows the TEM images of the FSP 4.5 vol.% CNT/2009Al composite and the CNTs extracted from the composite. The CNTs were singly dispersed in the aluminium matrix and randomly oriented (Fig. 4a). Damage of the CNTs during FSP was reported in our previous investigation [21] and it was found that the CNT structure damage was not severe. The average length of the CNTs extracted from the composite still remained above 400 nm, even after 4 pass FSP, as shown in Fig. 4b. Furthermore, HREM observations

indicated that the tube structure of CNTs in the composite was well retained and the CNT–Al interface was well bonded without void or defect (Fig. 4c).

Fig. 5 shows the grain microstructures of the T4-treated FSP 2009Al alloy, 1.5 vol.% and 4.5 vol.% CNT/2009Al composites. The average grain size of the 2009Al alloy was about 4 μm, whilst that of the 1.5 vol.% and 4.5 vol.% CNT/2009Al composites were 2 and 0.8 μm, respectively. Specifically, our previous investigation [21]

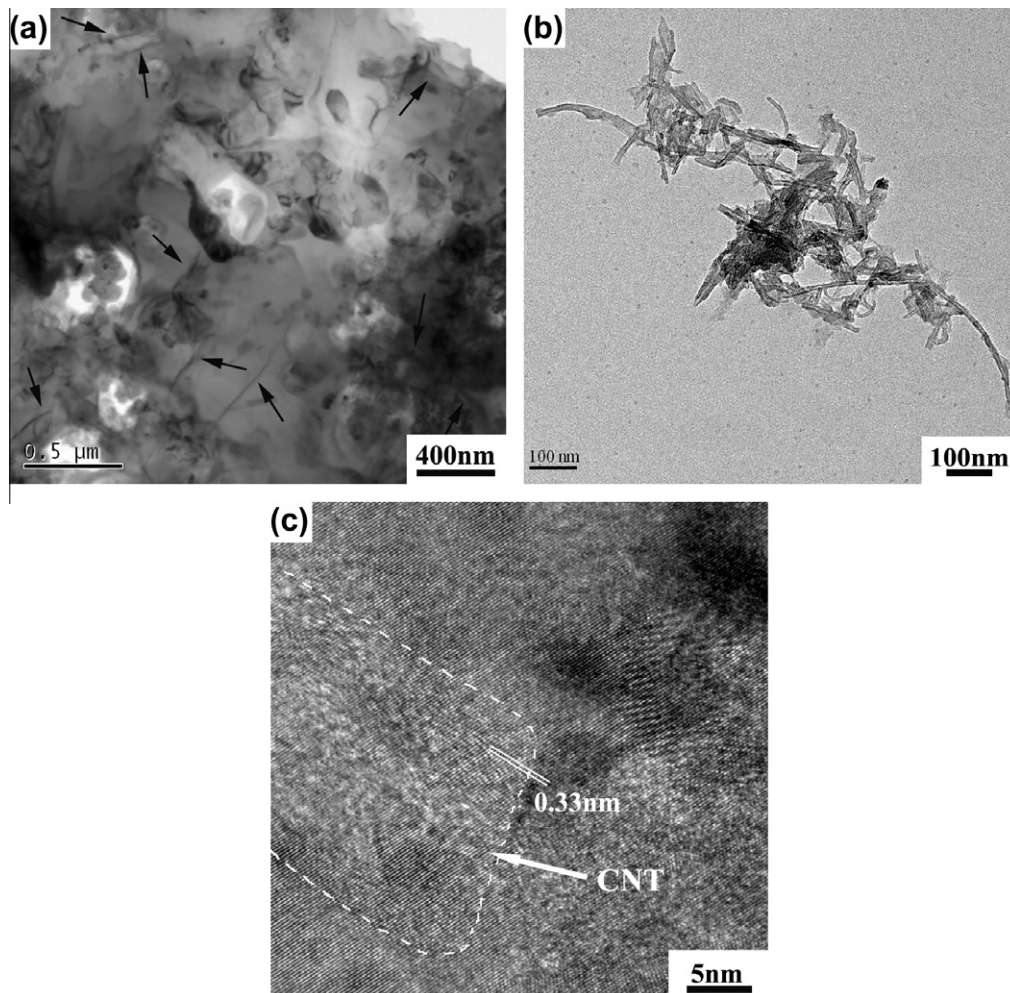


Fig. 4. (a) CNT distribution in aluminum matrix of FSP 4.5 vol.% CNT/2009Al composite, (b) CNTs extracted from composite and (c) HREM of CNT dispersed in aluminum matrix.

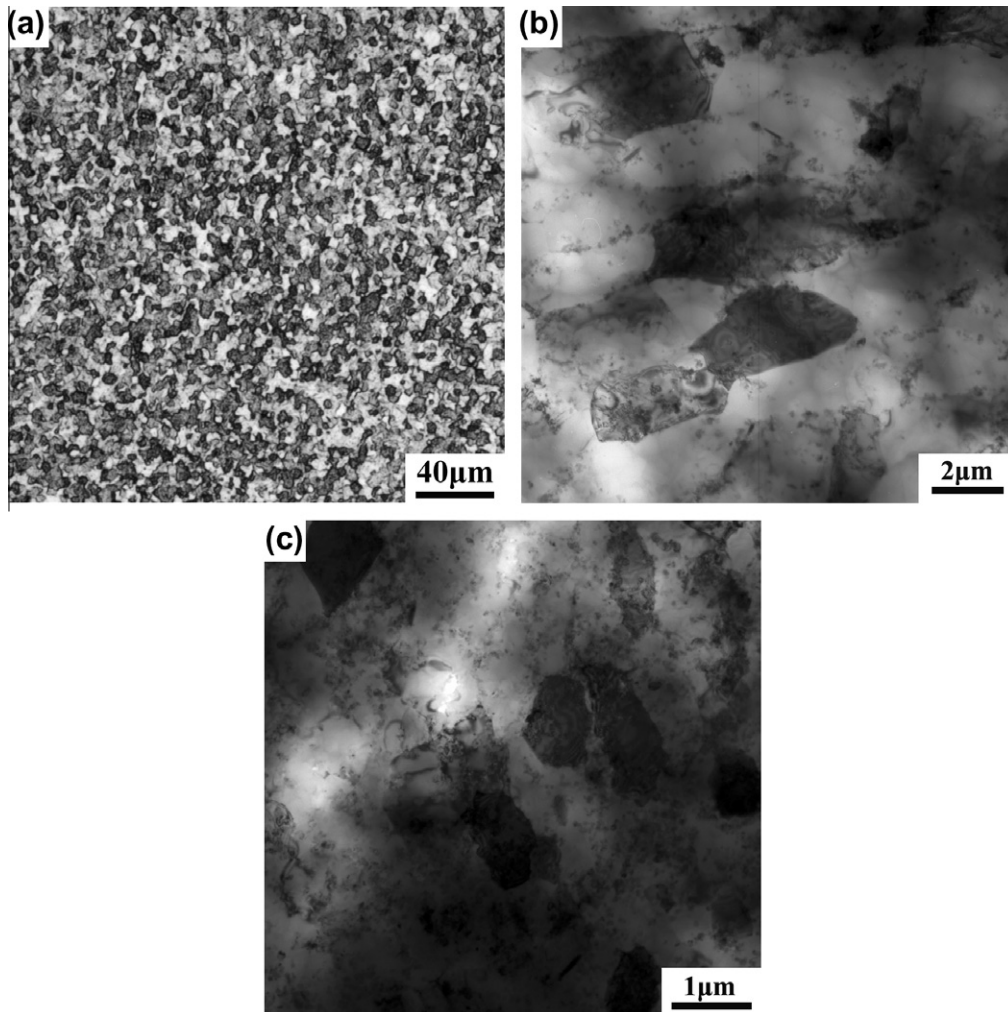


Fig. 5. Grain microstructure of (a) 2009Al, (b) 1.5 vol.% CNT/2009Al, and (c) 4.5 vol.% CNT/2009Al.

showed that in the 4.5 vol.% CNT/2009Al composite, the CNTs were often found at the boundaries of some even finer grains (~ 200 nm). This indicates that the nano-sized CNTs could exert an effective pinning on the grain boundaries, hindering the growth of the recrystallized grains during FSP and following solution-treatment. Thus, the CNT/2009Al composites showed a much finer grain size compared with the 2009Al alloy. This is in agreement with the result reported by Lipecka et al. [22]. They found that the CNTs enhanced the thermal stability of an ultrafine grained aluminium matrix. After annealing at 450°C ($0.7 T_m$) no evidence of grain growth was observed [22].

3.2. Tensile properties of the composites

Fig. 6 shows the tensile stress–strain curves of the FSP 2009Al alloy and CNT/2009Al composites at 293–573 K. Increasing the testing temperature led to a decreased strength level, for both matrix and CNT/2009Al composites. At room temperature (293 K), a “tip drop” phenomenon occurred on the stress–strain curves, for both the 1.5 vol.% CNT/2009Al and 4.5 vol.% CNT/2009Al composites, but not the 2009Al alloy and this could be attributed to the random orientation of the CNTs, i.e., the CNTs at some oriented directions might be preferentially de-bonded and thus a tip drop formed. At temperatures higher than 423 K, the tip drop phenomenon disappeared, mainly due to the fact that the stress loaded on the CNTs could not reach the critical stress value.

Fig. 7 shows the yield strength of the FSP composites at different temperatures. At temperatures from 293 to 573 K, the yield strength of the FSP 1.5 vol.% CNT/2009Al composite was enhanced compared with that of the 2009Al alloy. However, the strength enhancement at elevated temperatures was not as obvious as that at 293 K. For the FSP 4.5 vol.% CNT/2009Al composite, the yield strength showed different changes. At 293 K, the yield strength of the FSP 4.5 vol.% CNT/2009Al composite was much higher than that of the 2009Al alloy and 1.5 vol.% CNT/2009Al composite. As the temperature increased to 473 K, the yield strength of the 4.5 vol.% CNT/2009Al composite decreased significantly, to a level equivalent to that of the 1.5 vol.% CNT/2009Al composite. At 573 K, the yield strength of the 4.5 vol.% CNT/2009Al composite was even lower than that of the 2009Al alloy.

Figs. 8 and 9 show the fractographs of the FSP 1.5 vol.% CNT/2009Al composite and 4.5 vol.% CNT/2009Al composite at different temperatures. Two phenomena could be found on the fracture surfaces. Firstly, large numbers of uniformly dispersed CNTs were pulled out on the fracture surfaces of the 293 K tensile specimens. This means that no clustering existed in the composites. The detail that the CNTs on the fracture surfaces were identified as the pull-out CNTs has been reported in our previous study [21]. The numbers of the CNTs pulled out greatly decreased as the temperature increased to 573 K and only a few CNTs could be found on the fracture surfaces tested at 573 K. The pull-out length of the CNTs on the fracture surfaces at 573 K was also greatly reduced. Secondly,

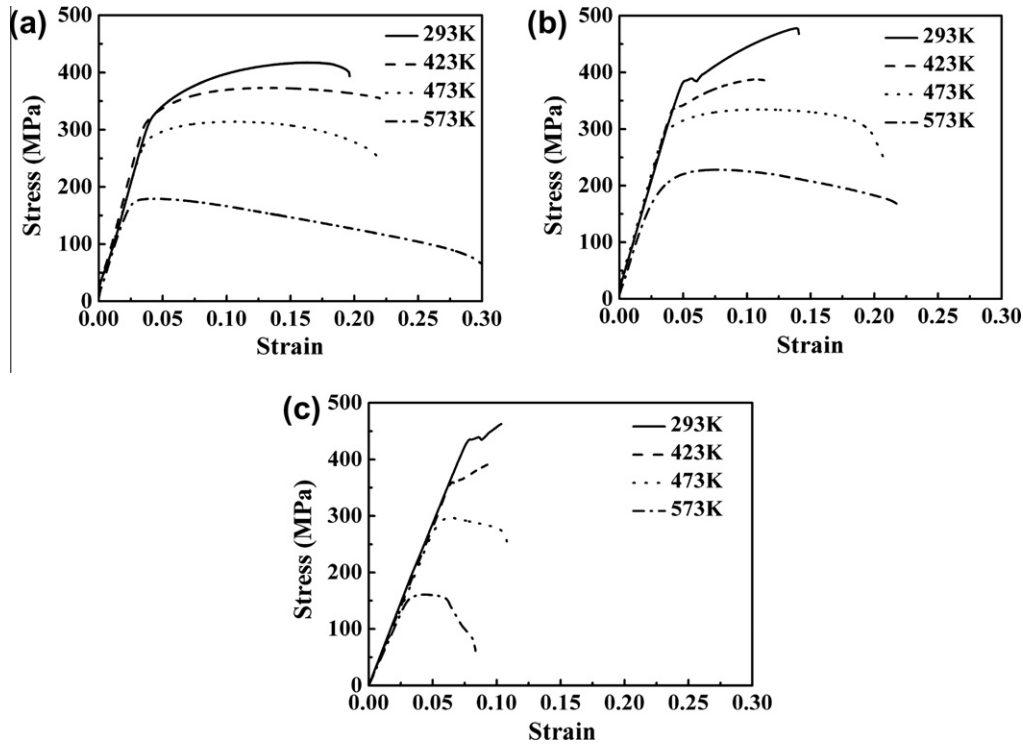


Fig. 6. Tensile curves of (a) 2009Al, (b) 1.5 vol.% CNT/2009Al, and (c) 4.5 vol.% CNT/2009Al at different temperatures.

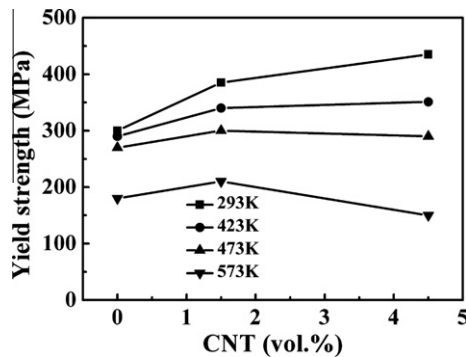


Fig. 7. Yield strength of CNT/2009Al composites tested at different temperatures.

as the testing temperature increased from 293 to 473 K, dimples became shallow. When the temperature reached 573 K, the composites showed an obvious intergranular fracture. These two phenomena mean that the fracture mode changed from the CNT pull-out to the grain boundary damage as the temperature increased from 293 to 573 K. This could also imply that the bonding strength of CNT–Al interface was still stronger than that of the aluminium matrix at temperatures of 293–573 K.

The enhanced strength for the CNT/Al composites results from two mechanisms. Firstly, the very fine grain size could strengthen the composite, especially at room temperature [23]. Secondly, the aspect ratio of the CNTs still remained larger than 20 after FSP, which implied that load transfer could still operate even at elevated temperatures. At 293 K, the very fine matrix grains contributed to the strengthening of the composites. However, this situation changed as the temperature increased to an equi-cohesive temperature [24], above which the grain boundaries are weaker than the grain inner. Thus, the strength increase of the 1.5 vol.% CNT/2009Al composite relative to the 2009Al alloy at 423–573 K, was not as obvious as that at 293 K, and for the 4.5 vol.% CNT/

2009Al composite with a finer grain size, the strength at 573 K was even lower than that of 2009Al alloy.

As mentioned in our previous investigation [21], the yield strength of the CNT/Al composites at room temperature could be expressed by:

$$\sigma_c = (\sigma_0 + kd^{-1/2})[V_f(s+4)/4 + (1 - V_f)] \quad (1)$$

where σ_0 is rationalised as a frictional stress, which could be simply considered as the strength of the alloy with coarse grains, d is the matrix grain size in the composite, k is the Hall–Petch slope, σ_c is the yield strength of the composite, s is the aspect ratio of CNTs (larger than 20), and V_f is the volume fraction of CNTs.

Eq. (1) predicts that the CNT–Al interface is stronger than the Al matrix. At room temperature, the yield strength of the 1.5 vol.% and 4.5 vol.% CNT/2009Al composites was 385 MPa and 435 MPa, respectively, close to the calculated values (372 MPa and 452 MPa, respectively). It implies that the bonding strength of the CNT–Al interface was strong enough to transfer load from the aluminium matrix to the CNTs.

Considering temperature effects on the Hall–Petch equation and load transfer efficiency, Eq. (1) is changed into:

$$\sigma_c = (\tau\sigma_0 + \eta kd^{-1/2})[V_f(s+4)/4 + (1 - V_f)] \quad (2)$$

where τ is the coefficient of the elevated temperature influence on the intragranular strength, η is the coefficient of the elevated temperature influence on strength increase due to grain refinement.

For the composites reinforced with short fibre or particle reinforcement, the interface between reinforcement and matrix has a great influence on the deformation behaviour of the composites. A weak reinforcement–matrix bonding would result in preferential crack initiation and propagation at the interfaces. At elevated temperatures of 423 and 473 K, the tensile curves still exhibited a hardening behaviour (Fig. 6b and c), this means that the bonding strength of the CNT–Al interface was still larger than the strength of the Al matrix at these temperatures. At 573 K, the length of the

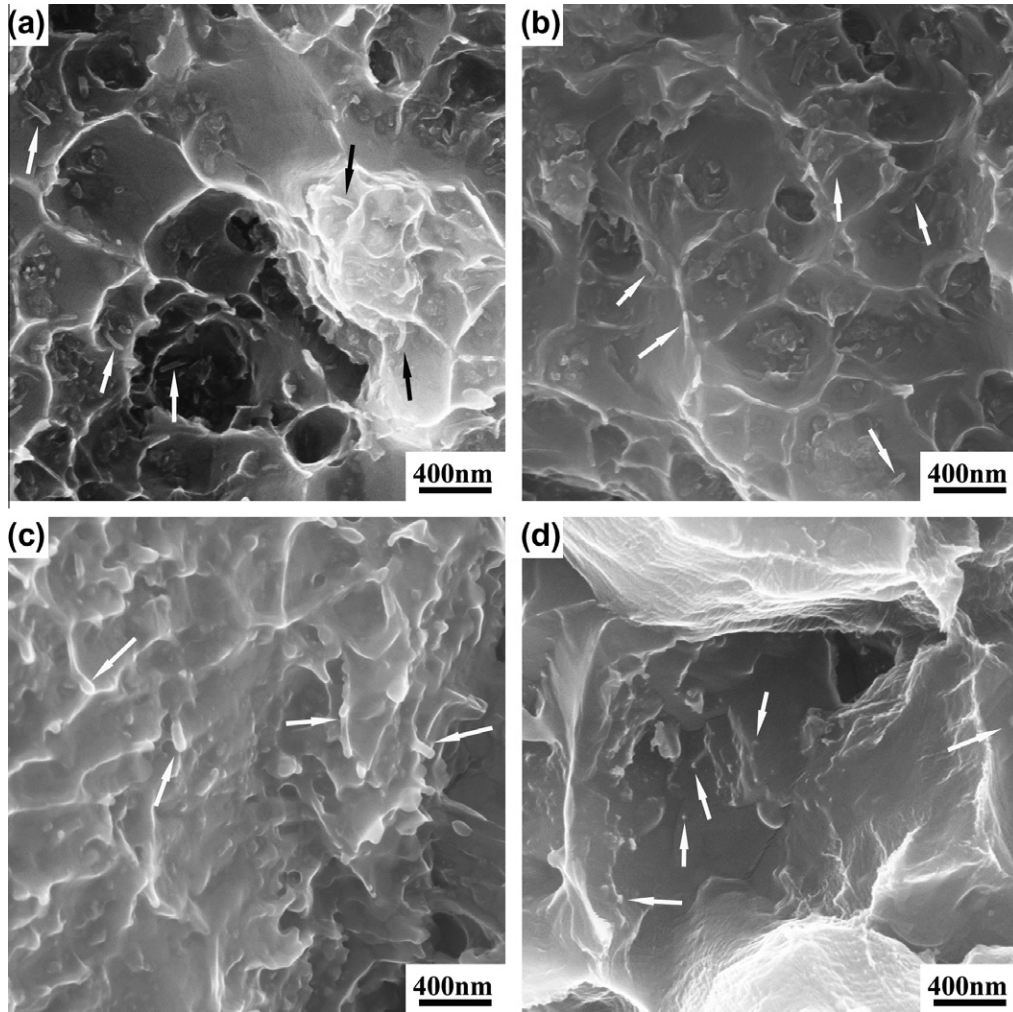


Fig. 8. Fractographs of 1.5 vol.% CNT/2009Al composite tested at different temperatures: (a) 293 K, (b) 423 K, (c) 473 K, and (d) 573 K.

pulled-out CNTs was very short and only the tips of CNTs could be found, this implies that the fracture mainly occurred at the Al matrix and the bonding strength of the CNT–Al interface was still stronger than the strength of the Al matrix.

The grain size of the FSP 1.5 vol.% and 4.5 vol.% CNT/2009Al composites was 2 and 0.8 μm, respectively. This means that the grain boundary fraction of the composite with 4.5 vol.% CNTs was more than that of the composite with 1.5 vol.% CNTs. Thus, the $(\tau\sigma_0 + \eta kd^{-1/2})$ value of the 4.5 vol.% CNT/2009Al composite decreased more quickly than that of the 1.5 vol.% CNT/2009Al composite. This could also be reflected by the fractographs in Figs. 8 and 9. However, the $[V_f(s+4)/4 + (1 - V_f)]$ value could be considered to be little changed as the CNT–Al interfaces were still strong. Thus, according to Eq. (2), the strength of the 4.5 vol.% CNT/2009Al composite decreased faster than that of the 1.5 vol.% CNT/2009Al composite. As a result, between 293 and 423 K, the yield strength of the 4.5 vol.% CNT/2009Al composite was higher than that of the 1.5 vol.% CNT/2009Al composite, but as the temperature increased above 473 K, the situation was reversed.

3.3. CTE of the composites

Fig. 10 shows the CTE of the CNT/2009Al composites. The CTE decreased significantly due to the incorporation of the CNTs. The CTE decreased by about 9.3% and 29%, respectively, for the 1.5 vol.% and 4.5 vol.% CNT/2009Al composites. This indicates that

the CNTs could effectively constrain the thermal expansion of the aluminium matrix in the temperature range from 293 to 473 K.

In order to understand the thermal expansion behaviour of the composites, it is important to compare the experimental results with theoretical predictions. Two models, the rule of mixtures (ROMs) and Schapery’s model [25], have been used to predict the CTE of the composites. According to the ROMs, the CTE of the composites can be calculated by:

$$\alpha_c = \alpha_{CNT}V_{CNT} + \alpha_M(1 - V_{CNT}) \quad (3)$$

According to Schapery’s model, the approximate CTE of the composites can be calculated by:

$$\alpha_c = \frac{E_{CNT}\alpha_{CNT}V_{CNT} + E_M\alpha_M(1 - V_{CNT})}{E_{CNT}V_{CNT} + E_M(1 - V_{CNT})} \quad (4)$$

where α_c , α_{CNT} , α_M are the CTE of the composites, CNTs and matrix alloy; E_{CNT} and E_M are the modulus of the CNTs and matrix alloy; V_{CNT} is an equivalent volume fraction of the CNTs.

The E_{CNT} and E_M values of 1 TPa and 76 GPa, respectively, and the α_{CNT} and α_M values of 0 and $23.6 \times 10^{-6} \text{ K}^{-1}$, respectively, were used for calculation. The results calculated by the ROMs and Schapery’s model are shown in Fig. 10a. It is clear that the ROMs largely overestimates the CTE, as the model ignores the restriction influence of the metal matrix. On the other hand, the predictions by Schapery’s model are in good agreement with the experimental results. The diameters of the CNTs were of the size of nanometers,

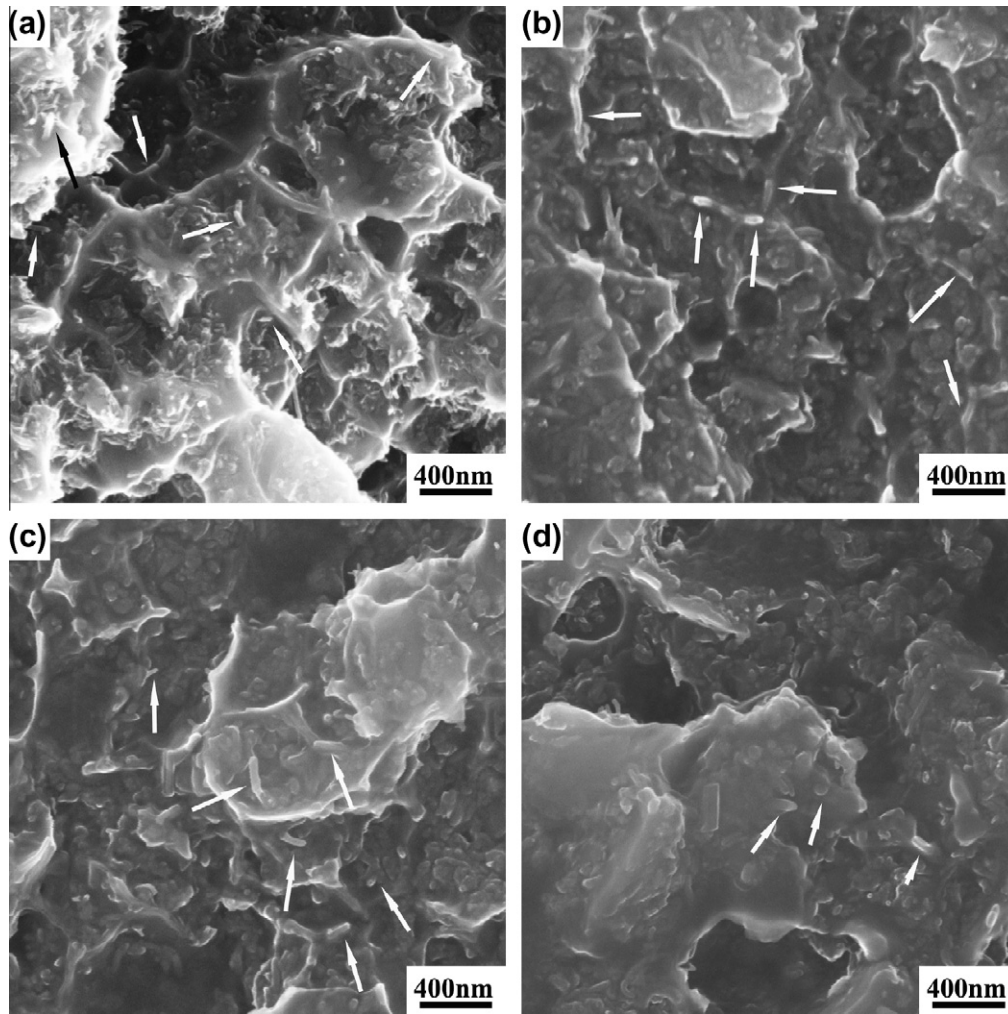


Fig. 9. Fractographs of 4.5 vol.% CNT/2009Al composite tested at different temperatures: (a) 293 K, (b) 423 K, (c) 473 K, and (d) 573 K.

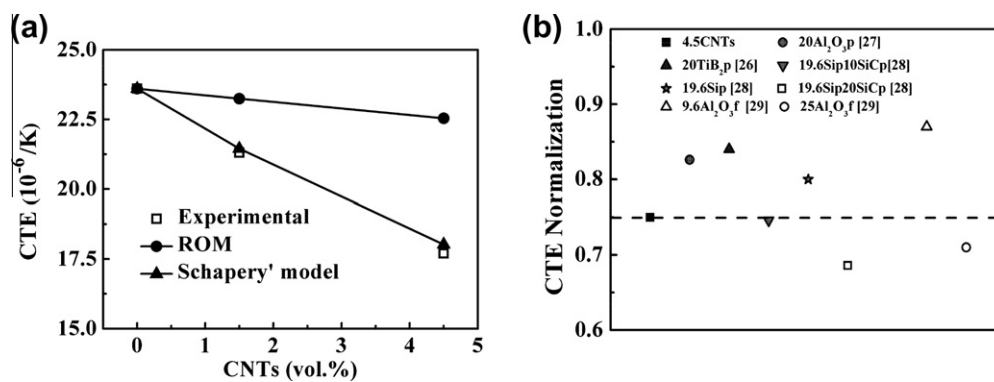


Fig. 10. (a) Comparison between experimental and calculated CTEs at 473 K for CNT/2009Al composites and (b) CTE comparison at 473 K between aluminium matrix composites reinforced by various reinforcements (the number before reinforcements was the volume fraction of reinforcements, p-particulate, f-short fibre).

which means that the CNTs had large surface areas. As discussed above, the elevated temperature tensile tests implied that the Al–CNT interfaces could still transfer load at the temperatures from 293 to 473 K. Thus, the specific surfaces of the CNTs were able to restrain the thermal strain during the temperature variation from 293 to 473 K.

For comparison, the CTEs of several composites reported by other researchers [26–29] are also shown in Fig. 10b. It is indicated that even a small amount of CNTs was effective in decreasing the

CTE of the composites compared with other particulates, or short fibres. This is mainly attributed to the large numbers of CNT–Al interfaces, the CTE value close to zero, and a high modulus of CNTs.

4. Conclusions

CNTs uniformly dispersed in the aluminium matrix by 4 pass FSP, could effectively hinder the grain growth of the matrix, thus

the grain sizes remained fine even after solution-treatment. Fine grain sizes contribute to the strengthening of the composites at room temperature, but this contribution decreases as the temperature is increased.

The yield strength of the 1.5 vol.% CNT/2009Al composite at 293–573 K was enhanced compared with that of the 2009Al alloy, which mainly resulted from load transfer mechanism.

At 293 K, the 4.5 vol.% CNT/2009Al composite exhibited significantly increased yield strength compared to the 2009Al alloy and 1.5 vol.% CNT/2009Al composite. However, the yield strength increase at 423–473 K was not as obvious as that at 293 K and particularly its yield strength at 573 K was even lower than that of the 2009Al alloy, mainly due to its finer grain size.

The CTE of the CNT/2009Al composites decreased when increasing the volume fraction of the CNTs, due to the large number of interfaces between the CNTs and aluminium matrix, which was in good agreement with the prediction by the Schapery's model.

Acknowledgements

The authors gratefully acknowledge the support of (a) the National Key Basic Research Program of China under Grant No. 2011CB932603 and 2012CB619600 and (b) the National Natural Science Foundation of China under Grant No. 50890171.

References

- [1] Krishnan A, Dujardin E, Ebbesen TW, Yianilos PN, Treacy MMJ. Young's modulus of single-walled nanotubes. *Phys Rev B* 1998;58(20):14013–9.
- [2] Wong EW, Sheehan PE, Lieber CM. Nanobeam mechanics: elasticity, strength, and toughness of nanorods and nanotubes. *Science* 1997;277(5334):1971–5.
- [3] Salvétat-Delmotte J-P, Rubio A. Mechanical properties of carbon nanotubes: a fiber digest for beginners. *Carbon* 2002;40(10):1729–34.
- [4] Poncharal P, Wang ZL, Ugarte D, De WA. Electrostatic deflections and electromechanical resonances of carbon nanotubes. *Science* 1999;283(5407):1513–6.
- [5] Qian D, Wagner GJ, Liu WK, Yu M-F, Ruoff RS. Mechanics of carbon nanotubes. *Appl Mech Rev* 2002;55(6):495–533.
- [6] Yosida Y. High-temperature shrinkage of single-walled carbon nanotube bundles up to 1600 K. *J Appl Phys* 2000;87(7):3338–41.
- [7] George R, Kashyap KT. Strengthening in carbon nanotube/aluminium (CNT/Al) composites. *Scripta Mater* 2005;53(10):1159–63.
- [8] Deng CF, Wang DZ. Processing and properties of carbon nanotubes reinforced aluminum composites. *Mater Sci Eng A* 2007;444(1–2):138–45.
- [9] Choi HJ, Kwon GB, Lee GY, Bae DH. Reinforcement with carbon nanotubes in aluminum matrix composites. *Scripta Mater* 2008;59(3):360–3.
- [10] Deng CF, Ma YX, Zhang P, Zhang XX, Wang DZ. Thermal expansion behaviors of aluminum composite reinforced with carbon nanotubes. *Mater Lett* 2008;62(15):2301–3.
- [11] Park JH, Alegaonkar PS, Jeon SY, Yoo JB. Carbon nanotube composite: dispersion routes and field emission parameters. *Compos Sci Technol* 2008;68(3–4):753–9.
- [12] Esawi AMK, Morsi K, Sayed A, Abdel Gawad A, Borah P. Fabrication and properties of dispersed carbon nanotube–aluminum composites. *Mater Sci Eng A* 2009;508(1–2):167–73.
- [13] Kondoh K, Fukuda H, Umeda J, Imai H, Fugetsu B, Endo M. Microstructural and mechanical analysis of carbon nanotube reinforced magnesium alloy powder composites. *Mater Sci Eng A* 2010;527(16–17):4103–8.
- [14] Kondoh K, Threrujirapapong T, Imai H, Umeda J, Fugetsu B. Characteristics of powder metallurgy pure titanium matrix composite reinforced with multi-wall carbon nanotubes. *Compos Sci Technol* 2009;69(7–8):1077–81.
- [15] Konya Z, Zhu J, Niesz K, Mehn D, Kiricsi I. End morphology of ball milled carbon nanotubes. *Carbon* 2004;42(10):2001–8.
- [16] Berbon PB, Bingel WH, Mishra RS, Bampton CC, Mahoney MW. Friction stir processing: a tool to homogenize nanocomposite aluminum alloys. *Scripta Mater* 2001;44(1):61–6.
- [17] Mishra RS, Ma ZY, Charit I. Friction stir processing: a novel technique for fabrication of surface composite. *Mater Sci Eng A* 2003;341(1–2):307–10.
- [18] Morisada Y, Fujii H, Nagaoka T, Fukusumi M. Nanocrystallized magnesium alloy–uniform dispersion of C₆₀ molecules. *Scripta Mater* 2006;55(11):1067–70.
- [19] Johannes LB, Yowell LL, Sosa E, Arepalli S, Mishra RS. Survivability of single-walled carbon nanotubes during friction stir processing. *Nanotechnology* 2006;17(12):3081–4.
- [20] Morisada Y, Fujii H, Nagaoka T, Fukusumi M. MWCNTs/AZ31 surface composites fabricated by friction stir processing. *Mater Sci Eng A* 2006;419(1–2):344–8.
- [21] Liu ZY, Xiao BL, Wang WG, Ma ZY. Singly dispersed CNTs in CNT/Al composite fabricated by powder metallurgy combined with friction stir processing. *Carbon* 2012;50(5):1843–52.
- [22] Lipecka J, Andrzejczuk M, Lewandowska M, Janczak-Rusch J, Kurzydowski KJ. Evolution of thermal stability of ultrafine grained aluminium matrix composites reinforced with carbon nanotubes. *Compos Sci Technol* 2011;71:1881–5.
- [23] Choi H, Shin J, Min B, Park J, Bae D. Reinforcing effects of carbon nanotubes in structural aluminum matrix nanocomposites. *J Mater Res* 2009;24(28):2610–6.
- [24] Nganbe M, Heilmaier M. High temperature strength and failure of the Ni-base superalloy PM 3030. *Int J Plast* 2009;25(5):822–37.
- [25] Clyne TW, Withers PJ. An introduction to metal matrix composites. England (Cambridge): Cambridge Univ Press, 1993. p. 120–3.
- [26] Tjong SC, Tam KF. Mechanical and thermal expansion behavior of hipped aluminum–TiB₂ composites. *Mater Chem Phys* 2006;97(1):91–7.
- [27] Park CS, Kim MH, Lee C. A theoretical approach for the thermal expansion behavior of the particulate reinforced aluminum matrix composite Part I: a thermal expansion model for composites with mono-dispersed spherical particles. *J Mater Sci* 2001;36(14):3579–87.
- [28] Park CS, Kim CH, Kim MH, Lee C. The effect of particle size and volume fraction of the reinforced phases on the linear thermal expansion in the Al–Si–SiCp system. *Mater Chem Phys* 2004;88(1):46–52.
- [29] Nassini HE, Moreno M. Thermal expansion behavior of aluminum alloys reinforced with alumina planar random short fibers. *J Mater Sci* 2001;36(11):2759–72.